

---

---

## ORIGINAL ARTICLE

---

---

# Dynamic Contrast-enhanced Magnetic Resonance Imaging Scan in Osteosarcoma and Ewing Sarcoma

OM Albtoush<sup>1</sup>, M Al-Hussaini<sup>2</sup>, S Yaser<sup>3</sup>, A Mansour<sup>1</sup>

<sup>1</sup>Department of Radiology, <sup>2</sup>Department of Pathology, <sup>3</sup>Department of Oncology, King Hussein Cancer Center, Amman, Jordan

### ABSTRACT

**Objective:** To compare the initial enhancement patterns in patients with osteosarcoma and Ewing sarcoma.

**Methods:** Patients diagnosed with osteosarcoma and Ewing sarcoma between June 2013 and July 2014 were included. Patients received dynamic contrast-enhanced magnetic resonance imaging scans in order to determine the initiation of enhancement time and the enhancement curve.

**Results:** In total, 19 of 21 (90%) patients with osteosarcoma showed earlier initiation of enhancement compared with five of 20 (25%) patients with Ewing sarcoma.

**Conclusion:** Patients with osteosarcoma showed more initial hypervascularity than did those with Ewing sarcoma, manifested by considerable differences in the percentage with early initiation of enhancement in the dynamic analysis.

**Key Words:** Magnetic resonance imaging/methods; Osteosarcoma; Sarcoma, Ewing

## 中文摘要

### 骨肉瘤和尤文氏肉瘤患者的動態對比增強磁共振成像結果比較

OM Albtoush、M Al-Hussaini、S Yaser、A Mansour

**目的：**比較骨肉瘤和尤文氏肉瘤患者的初始強化模式。

**方法：**在2013年6月至2014年7月期間診斷為骨肉瘤和尤文氏肉瘤的患者被納入研究。患者進行動態對比增強磁共振成像以確定初始強化時間和強化曲線。

**結果：**21例（90%）骨肉瘤中有19例顯示較早初始強化，同樣情況在尤文氏肉瘤中則有5例（25%）。

**結論：**基於動態分析顯示初始強化時間的比例差異，骨肉瘤的高血管供應較尤文氏肉瘤為多。

---

---

**Correspondence:** Dr OM Albtoush, Department of Radiology, King Hussein Cancer Center, Amman, Jordan.

Email: o.albtoush@yahoo.com

Submitted: 9 Feb 2017; Accepted: 10 Mar 2017.

Previous Presentation: An earlier version of this paper was presented as an EPOS poster presentation at ECR 2016, Vienna, Austria, 2-6 March 2016.

Disclosure of Conflicts of Interest: All authors have no conflict of interest to disclose.

Funding/Support: This research received no specific grant from any funding agency in the public, commercial, or not-for-profit sectors.

## INTRODUCTION

Osteosarcoma (OS) and Ewing sarcoma (ES) are among the most common primary malignant bone tumours in young patients. Both of these tumoural entities show unique epidemiological features, sites of predilection, and imaging characteristics, which can contribute to their diagnostic evaluation.

Magnetic resonance imaging (MRI) is used mainly for accurate assessment of tumoural extension and the presence of skip/metastatic deposits. Dynamic contrast-enhanced MRI (DCE-MRI) is an imaging technique for evaluation of tumoural vascularity based on signal alterations in correlation with the time progression after application of the contrast material. This imaging technique can be applied in several aspects, including tissue characterisation, local staging, biopsy guidance, monitoring of preoperative chemotherapy, detection of residual or recurrent tumour, and distinguishing tumoural tissue from fibrosis.<sup>1</sup> DCE-MRI has proven diagnostic value in differentiation of benign and malignant cartilaginous tumours with sensitivity of 89% and specificity of 84%.<sup>2</sup> DCE-MRI is also important for the evaluation of tumour recurrence at the surgical bed in postoperative patients.<sup>3</sup>

The present study analysed DCE-MRI scans of OS and ES looking for specific enhancement trends. These scans might carry a diagnostic relevance in addition to the well-known superiority of MRI scan in assessing tumoural extension. DCE-MRI scans might alter the understanding of the treatment response of both OS and ES. Prediction of the nature of the neoplastic process will be beneficial in cases of inconclusive histopathological results due to non-representative samples as well as in cases with small early tumoural presentation.

## METHODS

DCE-MRI scans were performed in patients with OS or ES newly diagnosed between June 2013 and July 2014. DCE-MRI was part of the routine patient scan. No additional informed consent for this scan was obtained from the patients. Approval was obtained from the institutional review board committee.

A total of 41 patients (30 male and 11 female) with histopathologically proven diagnosis of OS and ES and available preoperative DCE-MRI scans were included in the study. Of these, 38 (93%) patients had primary bone tumour and three (7%) patients had tumours of extra skeletal origin. Two patients with motion artefacts,

which interfered with the proper evaluation of the dynamic analysis, were excluded from the study.

Of the 41 patients included, 21 (51%) had OS and 20 (49%) had ES. The mean age of presentation for patients with ES was 15 (range, 4-30) years and that for patients with OS was 18 (range, 8-27) years.

MRI contrast medium administration was restricted to patients with good renal function. For patients >18 years, 0.2 mL/kg of 0.5 mmol/mL gadoversetamide was used as the contrast medium; for those aged ≤18 years, 0.2 mL/kg of 0.5 mmol/mL gadopentetate dimeglumine was used. The mean rate of injection was 1 to 2 mL/s, depending on patient status. The DCE-MRI protocol was applied using a 1.5-T MRI system (MAGNETOM Avanto; Siemens Medical Solutions, Erlangen, Germany) and a 3-T MRI system (Ingenia Release 4.1.3; Philips Medical Systems, Best, The Netherlands).

Conventional imaging techniques included a pre-contrast axial spin echo T1-weighted sequence, axial short-tau inversion recovery (STIR) in at least two orthogonal planes, a coronal T1-weighted sequence, and a STIR sequence with a large field of view (FOV) covering the two nearby joints. Post-contrast scans included a multiplanar T1-weighted sequence with fat saturation.

The DCE-MRI scans were acquired using three-dimensional T1-weighted gradient echo sequences starting just before the application of the contrast material and lasted for 2 minutes, composed of 40 runs with post-processing subtraction. The FOV was selected to cover the whole mass with an average of 16 slices. Mean slice thickness was 10 mm but varied according to tumour size. Imaging parameters used were: 130- to 300-mm FOV, 10-degree flip angle, TR/TE of 3.4/1.66 milliseconds, and a 128 × 256 matrix. The dynamic assessment comprised two parameters: determination of initiation of enhancement (IOE) time and drawing of the post-processing curve type. For optimal calculation of the IOE time and the enhancement curve, the region of interest was chosen by a radiologist experienced in musculoskeletal imaging.

The IOE time was calculated from the start of nearby arterial enhancement to the start of solid tumoural enhancement. Enhancement curves were drawn for each case with three reference points: earliest enhancing solid tumoural component, nearby enhancing artery, and muscle or subcutaneous region (Figure 1).

The enhancement curve type is described as exponential versus gradual, according to the trend of tumoural enhancement. If the slope of the tumoural enhancement curve is  $>60$  degrees it is described as exponential (Figure 2), whereas if it is  $\leq 60$  degrees it is considered as gradual (Figure 3).

The IOE times were available for all patients. Enhancement curves were available for only 39 patients (21 with OS and 18 with ES) due to technical difficulties. The results were interpreted by two consultant radiologists with 2 and 10 years of experience in oncological MRI scans, including musculoskeletal tumours.

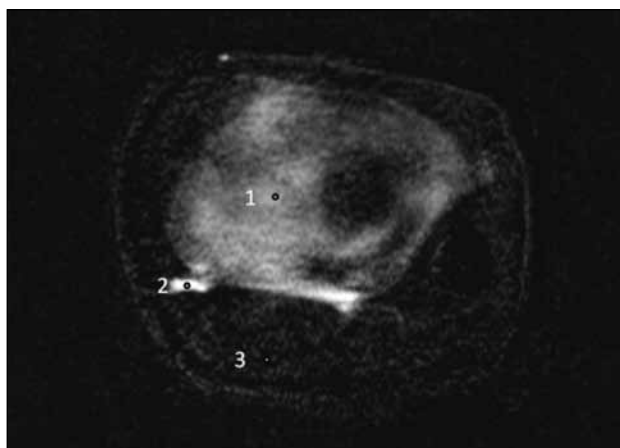


**Figure 1.** Drawing of the enhancement curve by selecting three points of reference: the enhancing solid tumoural component (1); the nearby arterial enhancement (2); and the baseline muscular enhancement (3).

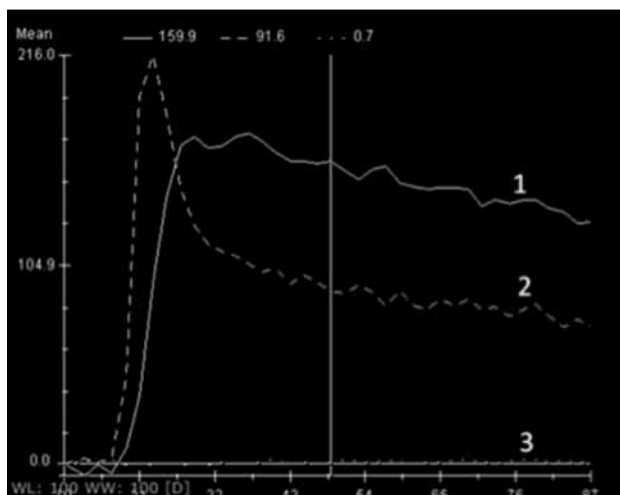


**Figure 2.** Exponential tumoural enhancement of the solid tumoural curve with a  $>60$ -degree slope. Three curves have been drawn: the solid tumoural curve (1); the nearby arterial curve (2); and the baseline curve (3).

## RESULTS

The IOE time for all patients is shown in Table 1. There were more patients with OS ( $n = 19$ ; 90%) showing earlier IOE time within the first scan after the nearby arterial enhancement or within the first 3 seconds (Figure 4) than patients with ES ( $n = 5$  [25%];  $P \leq 0.0001$ ).

From the enhancement curves, 11 (52%) patients with OS showed exponential enhancement whereas seven (39%) patients with ES showed exponential curve, resulting in a non-significant difference between the tumour types (Table 2).

The anatomical distribution of these cases, IOE times, and enhancement curve types are shown in Tables 3 and 4.

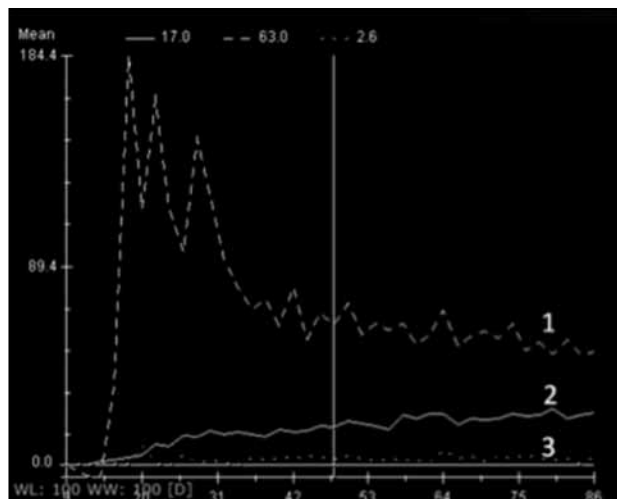


**Figure 3.** Gradual tumoural enhancement of the solid tumoural curve with a  $<60$ -degree slope. Three curves have been drawn: the arterial curve (1); the solid tumoural curve (2); and the baseline curve (3).

**Table 1.** Initiation of enhancement time for patients with osteosarcoma and Ewing sarcoma.

Time	Osteosarcoma (n = 21)	Ewing sarcoma (n = 20)
$\leq 3$ Seconds	19 (90%)	5 (25%)
$> 3$ Seconds	2 (10%)	15 (75%)

**Table 2.** Type of enhancement curve for patients with osteosarcoma and Ewing sarcoma.

Type	Osteosarcoma (n = 21)	Ewing sarcoma (n = 18)
Exponential	11 (52%)	7 (39%)
Gradual	10 (48%)	11 (61%)

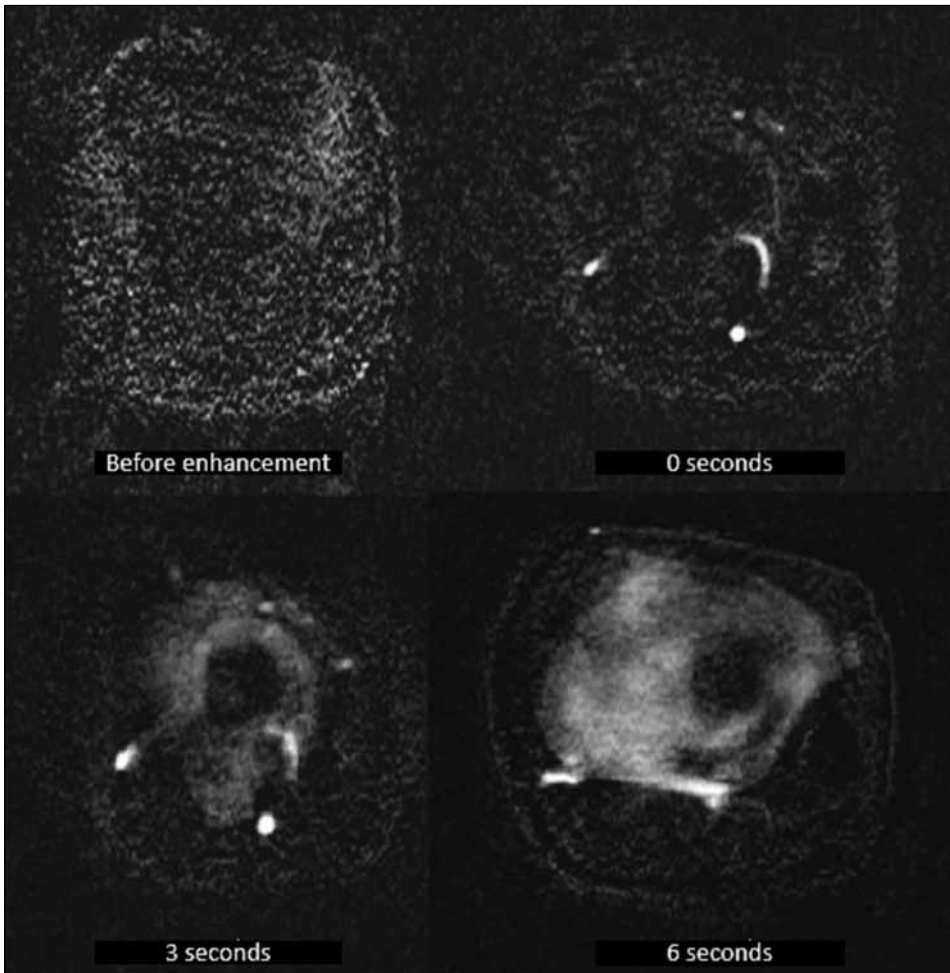


**Figure 4.** Dynamic contrast-enhanced magnetic resonance imaging scans before enhancement, at the start of nearby arterial enhancement (0 seconds), and at 3 and 6 seconds after enhancement. The solid tumoural component shows an early enhancement within 3 seconds after the nearby arterial enhancement.

**Table 3.** Anatomical distribution of cases of osteosarcoma.

Tumour location	Initiation of enhancement time (s)	Enhancement curve type
Humerus	3	Exponential
Tibia	3	Exponential
Fibula	3	Exponential
Femur	3	Gradual
Fibula	3	Gradual
Tibia	3	Gradual
Femur	3	Exponential
Humerus	3	Gradual
Radius	3	Exponential
Tibia	3	Exponential
Tibia	3	Exponential
Femur	9	Gradual
Femur	3	Exponential
Humerus	3	Exponential
Femur	3	Exponential
Femur	3	Gradual
Tibia	3	Gradual
Humerus	3	Exponential
Femur	3	Gradual
Femur	6	Gradual
Femur	3	Gradual

**Table 4.** Anatomical distribution of cases of Ewing sarcoma.

Tumour location	Initiation of enhancement time (s)	Enhancement curve type
Humerus	3	Exponential
Humerus	6	Not available
Radius	6	Exponential
Humerus	3	Gradual
Humerus	6	Gradual
Tibia	6	Exponential
Iliac	9	Gradual
Axilla	12	Gradual
Tibia	6	Gradual
Femur	6	Gradual
Foot	6	Gradual
Femur	3	Exponential
Iliac	6	Gradual
Iliac	9	Gradual
Shoulder	9	Not available
Scapula	6	Gradual
Thigh	18	Gradual
Pelvic	9	Exponential
Sacral	3	Exponential
Tibia	3	Exponential

## DISCUSSION

OS and ES are among the most common primary malignant bone tumours in young patients. In a large study from 1975 to 1995 that included approximately 14% of the population of the United States, OS and ES represented about 56% and 34% of primary malignant bone tumours in patients <20 years, respectively.<sup>4</sup>

There are unique epidemiological features and sites of predilection for both OS and ES, which can aid in tumour characterisation. Conventional radiography can reveal the size of the extraosseous component in relation to the osseous involvement, the type of periosteal reaction, and the type of matrix mineralisation, though in many cases these signs are non-specific. MRI is used mainly for accurate assessment of tumoural extension and for revealing the presence of skip/metastatic deposits in the covered FOV. Bone scintigraphy can reveal metastatic involvement in the whole skeleton.

DCE-MRI evaluates the tumour vascularity manifested by the increase in signal following administration of gadolinium-based MRI contrast material in T1-weighted gradient echo sequences with post-processing subtraction. Malignant lesions have been found to show higher enhancement as well as an increased rate of enhancement; however, there is an overlap in highly vascular benign lesions and malignant lesions.<sup>5</sup>

Kubo et al<sup>6</sup> found that OS and ES are more hypervascular than chondrosarcoma. Bajpai et al<sup>7</sup> demonstrated the role of DCE-MRI as a non-invasive imaging surrogate of tumour angiogenesis in OS. Angiogenesis has also been linked to the metastatic process. Mikulić et al<sup>8</sup> demonstrated that high tumour vascularity is predictive of a greater probability of distant metastasis and of shorter overall and disease-free survival.

In their review of the microvascular density in 25 OS patients, Ek et al<sup>9</sup> concluded that OS is a relatively vascular tumour. This increase in microvascular density is not age-related.<sup>10</sup> In a study by Mikulić et al,<sup>11</sup> the increased microvascular density of ES also did not correlate with outcome, although the microvascular density of OS was higher than that of ES.<sup>9,11</sup>

## CONCLUSION

There are considerable differences in the percentage of

cases with early IOE time in both OS and ES, suggesting that OS has more initial hypervascularity than does ES. These results show a significant diagnostic difference between both tumours using dynamic MRI scan. In addition to the well-known superiority of MRI in assessing tumoural extension, DCE-MRI may allow a better understanding of treatment response in both OS and ES.

## ACKNOWLEDGMENT

The current research paper was made possible through the help and support of senior MRI technician Ahmad Al Gharib and statistician Dalia Al-Rimawi from the Biostatistics Unit of the Research Office, King Hussein Cancer Center.

## REFERENCES

1. Costa FM, Canella C, Gasparetto E. Advanced magnetic resonance imaging techniques in the evaluation of musculoskeletal tumors. *Radiol Clin North Am.* 2011;49:1325-58,vii-viii. [Crossref](#)
2. Geirnaerd MJ, Hogendoorn PC, Bloem JL, Taminiau AH, van der Woude HJ. Cartilaginous tumors: fast contrast-enhanced MR imaging. *Radiology.* 2000; 214:539-46. [Crossref](#)
3. Shapeero LG, Vanel D. MR imaging in the follow-up evaluation of aggressive soft tissue tumors. *Semin Musculoskelet Radiol.* 1999;3:197-206. [Crossref](#)
4. Ries LA, Smith MA, Gurney JG, Linet M, Tamra T, Young JL, et al, editors. *Cancer Incidence and Survival among Children and Adolescents: United States SEER Program 1975-1995* (NIH Pub. No. 99-4649). Bethesda, MD: National Cancer Institute, SEER Program; 1999. p 99-110.
5. Verstraete KL, De Deene Y, Roels H, Dierick A, Uyttendaele D, Kunnen M. Benign and malignant musculoskeletal lesions: dynamic contrast-enhanced MR imaging — parametric “first-pass” images depict tissue vascularization and perfusion. *Radiology.* 1994;192:835-43. [Crossref](#)
6. Kubo T, Shimose S, Fujimori J, Arihiro K, Ochi M. Diversity of angiogenesis among malignant bone tumors. *Mol Clin Oncol.* 2013;1:131-6. [Crossref](#)
7. Bajpai J, Gamanagatti S, Sharma MC, Kumar R, Vishnubhatla S, Khan SA, et al. Noninvasive imaging surrogate of angiogenesis in osteosarcoma. *Pediatr Blood Cancer.* 2010;54:526-31.
8. Mikulić D, Ilić I, Cepulić M, Orlić D, Giljević JS, Fattorini I, et al. Tumor angiogenesis and outcome in osteosarcoma. *Pediatr Hematol Oncol.* 2004;21:611-9. [Crossref](#)
9. Ek ET, Ojaimi J, Kitagawa Y, Choong PF. Does the degree of intratumoural microvessel density and VEGF expression have prognostic significance in osteosarcoma? *Oncol Rep.* 2006;16:17-23. [Crossref](#)
10. Ek ET, Ojaimi J, Kitagawa Y, Choong PF. Outcome of patients with osteosarcoma over 40 years of age: is angiogenesis a marker of survival? *Int Semin Surg Oncol.* 2006;3:7. [Crossref](#)
11. Mikulić D, Ilić I, Cepulić M, Giljević JS, Orlić D, Zupancić B, et al. Angiogenesis and Ewing sarcoma — relationship to pulmonary metastasis and survival. *J Pediatr Surg.* 2006;41:524-9. [Crossref](#)